Structure of RbFeO$_2$, refined from a reticular pseudomerohedrally twinned crystal with six domains

Jürgen Nuss, Naveed Zafar Ali and Martin Jansen

Structure of RbFeO₂, refined from a reticular pseudomerohedrally twinned crystal with six domains

Jürgen Nuss, Naveed Zafar Ali and Martin Jansen*

Max-Planck-Institut für Festkörperforschung, Heisenbergstrasse 1, D-70569 Stuttgart, Germany

Correspondence e-mail: m.jansen@fkf.mpg.de

$RbFeO_2$, rubidium oxoferrate, crystallizes as an orthorhombic structure. The crystals under investigation were composed of six individuals representing reticular pseudomerohedral twins with a pseudocubic twin lattice of index 4 because of the approximate equations $a(8)^{1/2} = b(2)^{1/2} = c$. The compound is isostructural with $KFeO_2$ ($KGaO_2$ type of structure) and is composed of $[FeO_{4/2}]^-$ corner-sharing tetrahedra, forming a three-dimensional cristobalite-like network, with Rb^+ ions occupying its interstices.

1. Introduction

Alkali metal oxoferrates(III) are known to form the family of composition $AFeO_2$, with A = Li (Tabuchi *et al.*, 1998), Na (Bertaut & Blum, 1954), K (Tomkowicz & Szytuła, 1977), Rb (Hoppe, 1965*a,b*) or Cs (Frisch & Röhr, 2004). With the exception of $LiFeO_2$ and α-$NaFeO_2$, all of them crystallize in stuffed-structure variants of β-cristobalite. They thus belong to the structure family of feldspars that displays an intriguing richness of twinning and disorder phenomena (Cahn, 1954; Smith & Brown, 1988). $CsFeO_2$ crystallizes as cubic in the $CsAlO_2$ type of structure [space group $Fd\bar{3}m$, a = 8.392 (2) Å]; $RbFeO_2$ (a = 8.10 Å) was reported to be isotypic with $CsFeO_2$; and $KFeO_2$, first assigned to the $CsAlO_2$ structure type with a = 7.99 Å (Barth, 1935), was later found to be orthorhombic [space group $Pbca$, a = 5.619 (3), b = 11.253 (6), c = 15.87 (1) Å], adopting the $KGaO_2$ type of structure (Pistorius & Vries, 1973).

Vielhaber & Hoppe (1969) found that $KGaO_2$ and $RbGaO_2$ are pseudocubic, with the actual structure being ortho-rhombic, with $a:b:c \simeq 1:2:3$. Corresponding to the similarity between the ionic radii of Fe^{3+} and Ga^{3+}, $KFeO_2$ also has this structure and one would expect $RbFeO_2$ to also be isostructural. In order to verify this assumption we synthesized $RbFeO_2$ with the help of the azide nitrate route (Trinschek & Jansen, 1999*a,b*), whereupon the crystal structure analysis was performed.

2. Experimental

2.1. Synthesis

$RbFeO_2$ was prepared *via* the azide/nitrate route (Trinschek & Jansen, 1999*a,b*) from $RbNO_3$ (Johnson Matthey, 99%), rubidium azide and iron oxide (Fe_2O_3). Rubidium azide was synthesized from aqueous HN_3 and rubidium carbonate. Iron(III) oxide, Fe_2O_3, was prepared by heating $FeC_2O_4 \cdot 2H_2O$ in a flow of oxygen at 623 K for 20 h. The phase purity of the precursors was monitored by X-ray analysis.

Table 1
Experimental details.

Crystal data

Chemical formula	FeO_2Rb
M_r	173.32
Cell setting, space group	Orthorhombic, *Pbca*
Temperature (K)	298 (2)
a, b, c (Å)	5.7568 (7), 11.5136 (13), 16.2827 (18)
V (Å^3)	1079.2 (2)
Z	16
D_x (Mg m^{-3})	4.267
Radiation type	Mo $K\alpha$
μ (mm^{-1})	23.21
Crystal form, colour	Block, black
Crystal size (mm)	$0.25 \times 0.20 \times 0.20$

Data collection

Diffractometer	SMART APEX II, Bruker AXS
Data collection method	ω scans
Absorption correction	Multi-scan (based on symmetry-related measurements)
T_{min}	0.005
T_{max}	0.011
No. of measured, independent and observed reflections	89 193, 14 009, 8087
Criterion for observed reflections	$I > 2\sigma(I)$
θ_{max} (°)	37.3

Refinement

Refinement on	F^2
$R[F^2 > 2\sigma(F^2)]$, $wR(F^2)$, S	0.053, 0.126, 1.17
No. of reflections	14 009
No. of parameters	78
Weighting scheme	$w = 1/[\sigma^2(F_o^2) + (0.0154P)^2 + 5.2299P]$, where $P = (F_o^2 + 2F_c^2)/3$
$(\Delta/\sigma)_{max}$	0.002
$\Delta\rho_{max}$, $\Delta\rho_{min}$ (e Å^{-3})	1.70, −1.86

Computer programs used: *APEX Suite* and *SAINT*32 (Bruker AXS, 2005), *SHELXS*97 (Sheldrick, 1997*a*), *SHELXL*97 (Sheldrick, 1997*b*), *ATOMS* (Dowty, 2005).

The starting materials were mixed in the ratio required according to (1), ground thoroughly in an agate mortar, pressed into pellets (Ø = 6 mm) under 10^5 N, dried in vacuum (10^{-3} mbar) at 400 K for 12 h and placed under argon into a tightly closed steel vessel, provided with a silver inlay (Sofin, Friese *et al.*, 2002; Sofin, Peters & Jansen, 2002).

$$5RbN_3 + RbNO_3 + 3Fe_2O_3 \rightarrow 6RbFeO_2 + 8N_2 \quad (1)$$
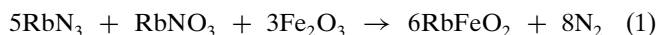
In a flow of dry argon the following temperature profile was applied: 298 → 533 K (100 K h^{-1}); 533 → 653 K (5 K h^{-1}); 653 → 793 K (20 K h^{-1}) with subsequent annealing for 50 h at 793 K. The reaction product was later cooled down slowly to 693 K (5 K h^{-1}) and then to room temperature at a rate of 100 K h^{-1}.

The black powder obtained is very sensitive to humid air and must be handled in an inert atmosphere. Single crystals have been grown by post annealing the reaction product at 783 K for 800 h. For this purpose, the microcrystalline primary product was pressed into pellets and placed in silver crucibles, closed with a silver stopper. The crucibles were sealed in glass ampoules under dried argon.
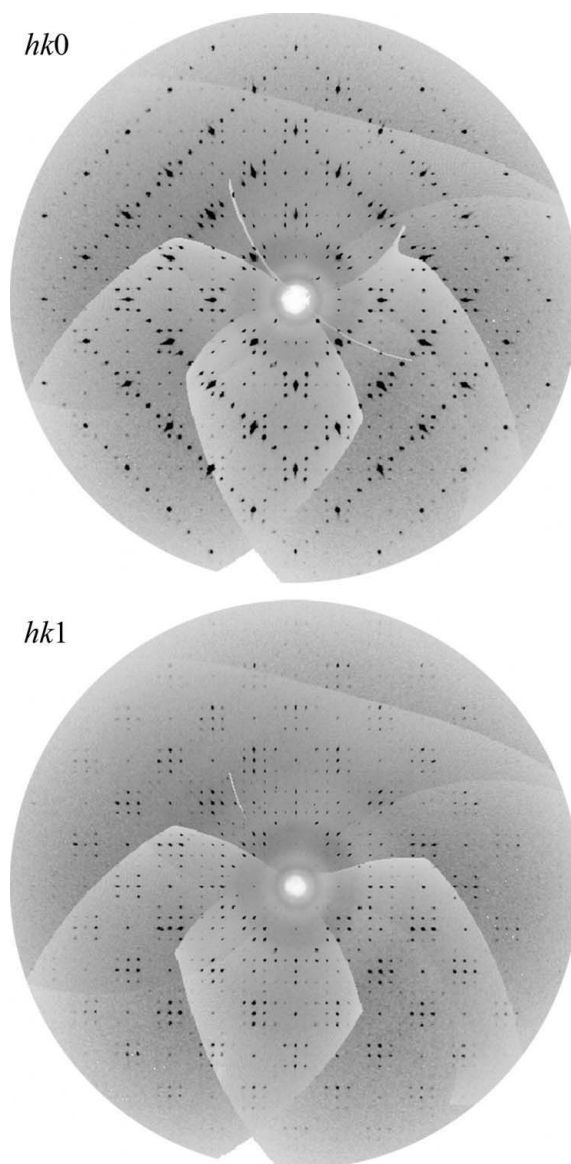

Figure 1
Reciprocal layers *hk*0 and *hk*1 (referring to twin domain I) constructed pixel by pixel from the original CCD frames.

2.2. X-ray diffraction

Two single crystals were selected in a drybox (M. Braun, Garching, Germany) under an argon atmosphere (< 0.1 p.p.m. O_2, H_2O) and mounted in sealed glass capillaries. Diffraction intensities were collected with a SMART APEX II three-cycle diffractometer equipped with an APEX II CCD detector (Bruker AXS). Experimental details for one of the crystals are given in Table 1; atomic coordinates have been deposited.[1]

3. Structure determination

The diffraction intensities of the first investigated crystal of RbFeO$_2$ could be indexed and integrated on the basis of the

[1] Supplementary data for this paper are available from the IUCr electronic archives (Reference: BP5004). Services for accessing these data are described at the back of the journal.
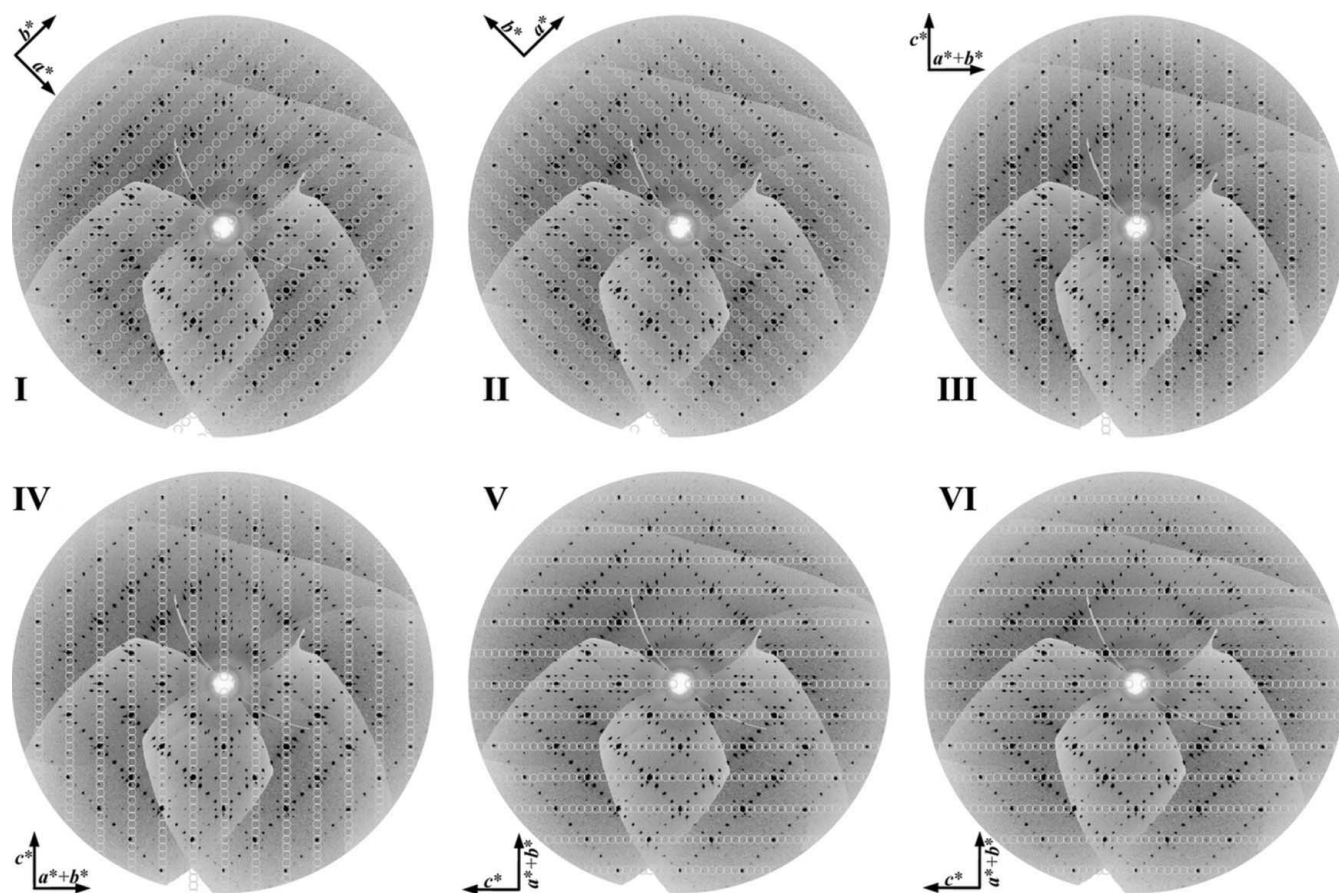
Figure 2
Reciprocal layer $hk0$ (referring to twin domain I). The reflections of the corresponding domains are emphasized by circles: $h\,k\,0$ for domains I and II, $h\,-2h\,l$ for domain III–VI. The directions of the reciprocal axes of each domain are drawn in.

cubic crystal system with $a_{\text{cubic}} = 16.283\,(2)$ Å ($R_{\text{int}} = 0.097$). This is an eightfold unit cell with doubled a axis compared with *e.g.* $CsFeO_2$ (Frisch & Röhr, 2004). No peak-splitting is observed with Mo $K\alpha$ radiation; Fig. 1 shows the zeroth and first layer of the reciprocal space of the first crystal under investigation, constructed pixel by pixel from the original CCD frames using the *Precession* module of the *Bruker Suite* software package (Bruker AXS, 2005). This procedure allows a detailed exploration of the reciprocal space, without restrictions to integer hkl values. The observed extinction rules $h00$: $h = 2n$; $0k0$: $k = 2n$; $00l$: $l = 2n$ lead to the space groups $P2_13$ (No. 198) and $P4_232$ (No. 208). Only in $P2_13$ could the heavy atoms be located, forming a three-dimensional network of two interpenetrating diamond-like structures, consisting of rubidium and iron, exclusively. Displacement parameters which were much too high were obtained during the structure refinement and no O atoms could be localized in the difference-Fourier map. The second crystal under investigation with $R_{\text{int}} \simeq 0.35$ for the cubic symmetry revealed that both crystals showed a special kind of twinning with different volume fractions of the twin individuals.

The structure of $KGaO_2$ (Vielhaber & Hoppe, 1969) is known to be an ordered variant of the $CsAlO_2$ type. The latter one represents a stuffed undistorted β-cristobalite type ($a = $

Table 2
Statistics of the measured reflections.

	Measured	Unique
Domain I only	6940	785
Domain II only	6960	785
Domain III only	6972	788
Domain IV only	6948	785
Domain V only	6955	786
Domain VI only	6954	785
Two domains	30 597	3654
Three domains	13 491	5286
Six domains	3376	1328
Sum	89 193	14 982

8.098 Å). The structure of $KGaO_2$ is orthorhombic with the space group $Pbca$. The unit cell contains 16 formula units with lattice constants related to the $CsAlO_2$ type of structure according to (2)

$$a \simeq a(CsAlO_2)/(2)^{1/2},$$
$$b \simeq a(CsAlO_2)(2)^{1/2},$$
$$c \simeq 2a(CsAlO_2). \qquad (2)$$

Starting from the cubic lattice of $CsAlO_2$, there are six possible orientations which can be chosen for the orthorhombic system. The six transformation matrices are given as:

$$\begin{pmatrix} \frac{1}{2} & 1 & 0 \\ -\frac{1}{2} & 1 & 0 \\ 0 & 0 & 2 \end{pmatrix} \quad \begin{pmatrix} \frac{1}{2} & 1 & 0 \\ \frac{1}{2} & -1 & 0 \\ 0 & 0 & -2 \end{pmatrix}$$

$$\begin{pmatrix} 0 & 0 & 2 \\ \frac{1}{2} & 1 & 0 \\ -\frac{1}{2} & 1 & 0 \end{pmatrix} \quad \begin{pmatrix} 0 & 0 & -2 \\ \frac{1}{2} & 1 & 0 \\ \frac{1}{2} & -1 & 0 \end{pmatrix}$$

$$\begin{pmatrix} \frac{1}{2} & 1 & 0 \\ 0 & 0 & 2 \\ -\frac{1}{2} & 1 & 0 \end{pmatrix} \quad \begin{pmatrix} \frac{1}{2} & 1 & 0 \\ 0 & 0 & -2 \\ \frac{1}{2} & -1 & 0 \end{pmatrix}.$$

These matrices were used to create a multi-component hkl file from the raw data set of the $RbFeO_2$ crystal during the integration procedure with the *Bruker Suite* software package (Bruker AXS, 2005), which can be used with the HKLF 5 option in *SHELXL* (Sheldrick, 1997*b*). The twinning matrices to transform the orthorhombic unit cells into each other are

$$\begin{pmatrix} 1 & 0 & 0 \\ 0 & 1 & 0 \\ 0 & 0 & 1 \end{pmatrix} \quad \begin{pmatrix} 0 & 2 & 0 \\ \frac{1}{2} & 0 & 0 \\ 0 & 0 & -1 \end{pmatrix}$$

$$\begin{pmatrix} \frac{1}{2} & -1 & 2 \\ -\frac{1}{4} & \frac{1}{2} & 1 \\ -\frac{1}{4} & -\frac{1}{2} & 0 \end{pmatrix} \quad \begin{pmatrix} \frac{1}{2} & -1 & -2 \\ -\frac{1}{4} & \frac{1}{2} & -1 \\ \frac{1}{4} & \frac{1}{2} & 0 \end{pmatrix}$$

$$\begin{pmatrix} \frac{1}{2} & 1 & -2 \\ \frac{1}{4} & \frac{1}{2} & 1 \\ \frac{1}{4} & -\frac{1}{2} & 0 \end{pmatrix} \quad \begin{pmatrix} \frac{1}{2} & 1 & 2 \\ \frac{1}{4} & \frac{1}{2} & -1 \\ -\frac{1}{4} & \frac{1}{2} & 0 \end{pmatrix}.$$

The reflection intensities were corrected for absorption and analyzed with the program *TWINABS* (Sheldrick, 2007). The analysis (Table 2) indicates that from all reflections (I_{all}) of *e.g.* domain I, $I_{all}/4$ belong to this domain exclusively, $3I_{all}/8$ belong to two domains, $I_{all}/4$ belong to three domains and $I_{all}/8$ belong to all six domains. This confirms that the special relations of the lattice constants lead to a reticular pseudo-merohedral twin: only a partial number (*reticular*) of the reflections are overlapping completely in three dimensions (*merohedral*). There are either completely overlapping or non-overlapping reflections, but no partially overlapping ones, as observed for *e.g.* dovetail twins. The twin lattice is *pseudo*-cubic because of
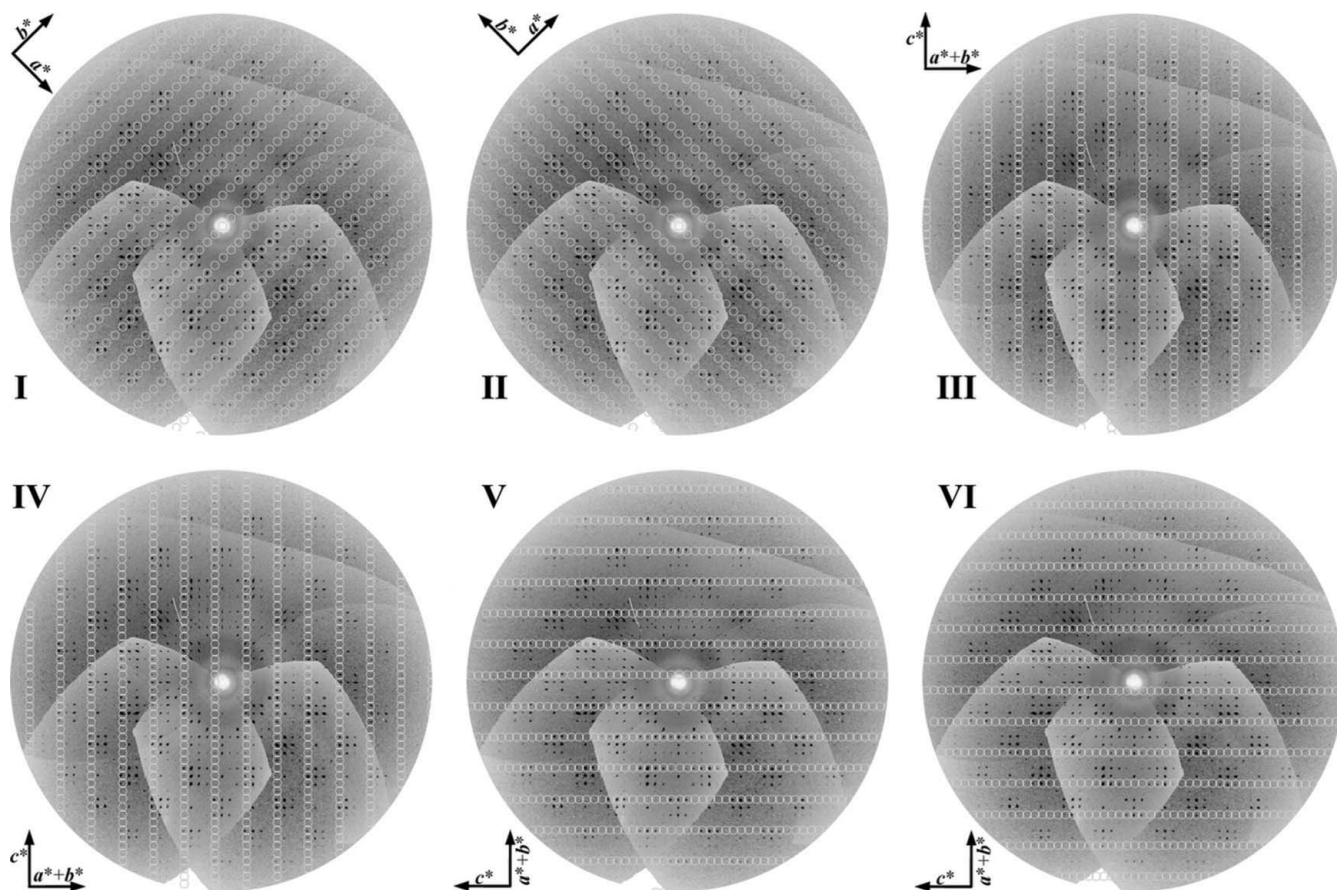

Figure 3
Reciprocal layer $hk1$ (referring to twin domain I). The reflections of the corresponding domains are emphasized by circles: $h\,k\,1$ for domain I and II, $h\,-2h+1\,l$ for domain III, $h\,2h-1\,l$ for domain IV, $h\,2h+1\,l$ for domain V and $h\,-2h-1\,l$ for domain VI. The directions of the reciprocal axes of each domain are drawn in.

Table 3
Selected bond distances and angles (Å, °).

| Fe1—O1	1.853 (3)	Rb1—O1	3.373 (4)
Fe1—O2	1.854 (3)	Rb1—O2	2.973 (3)
Fe1—O4	1.851 (3)	Rb1—O4	2.845 (3)
	1.869 (3)	Rb2—O1	2.961 (3)
Fe2—O1	1.843 (3)		3.159 (4)
Fe2—O2	1.865 (3)		3.207 (4)
Fe2—O3	1.861 (3)	Rb2—O2	3.000 (3)
	1.862 (3)	Rb2—O3	3.030 (3)
Rb1—O2	2.865 (3)	Rb2—O4	2.995 (3)
Rb1—O3	2.855 (3)		3.321 (3)
	3.279 (3)		3.345 (3)
	3.409 (3)		
O1—Fe1—O2	108.5 (1)	O1—Fe2—O3	113.0 (2)
O1—Fe1—O4	108.5 (2)	O2—Fe2—O3	107.4 (1)
	112.3 (2)		108.0 (1)
O2—Fe1—O4	110.1 (1)	O3—Fe2—O3	110.2 (1)
	108.9 (1)	Fe1—O1—Fe2	149.8 (2)
O4—Fe1—O4	108.6 (1)	Fe1—O2—Fe2	140.2 (2)
O1—Fe2—O2	108.0 (1)	Fe2—O3—Fe2	144.7 (2)
O1—Fe2—O3	110.1 (2)	Fe1—O4—Fe1	140.9 (2)

the approximate equations $a(8)^{1/2} = b(2)^{1/2} = c$, and the twin lattice index is $[j] = V_{cubic}/V_{ortho} = 4$ [$V_{cubic} = 4137.2$ (2) Å³, *cf.* Table 1; Hahn & Klapper, 2003]. Figs. 2 and 3 show the zeroth and first reciprocal layer with the reflections of each domain highlighted. It is shown that all the visible intensities are indexed by at least one of the six twinning domains, and the 'empty' reciprocal space is left unindexed.

The intensities, belonging to one domain only are not affected by the twinning and they have been used for structure solution. This solution yielded the positions of the heavy atoms Rb and Fe. With the complete data set, including all six domains, it was possible to locate the O atoms *via* a difference-Fourier synthesis. All atoms were refined anisotropically and the resulting twin volume fractions showed reasonable values in the order of magnitude of 1/6 for all six domains [respective volume fractions are $t1 = 0.1728$ (6); $t2 = 0.1970$ (6); $t3 = 0.1565$ (6); $t4 = 0.1472$ (6); $t5 = 0.1966$ (6); $t6 = 0.1299$ (6)].

4. Crystal structure and discussion

As already mentioned, RbFeO₂ crystallizes in the KGaO₂ type of structure. The essential feature of this structure is a three-dimensional network of corner-sharing $[FeO_{4/2}]^-$ tetrahedra with the monovalent ions located in large spaces in-between. As a consequence, both heavy atoms form a three-dimensional network of two interpenetrating diamond-like structures (NaTl structure type) built up by Rb and Fe, exclusively (Figs. 4 and 5). The $^3_\infty[FeO_{4/2}]^-$ framework corresponds to $^3_\infty[SiO_{4/2}]$ in β-cristobalite. The Fe—O bond distances lie in a narrow range and are in good agreement with the sum of the ionic radii. The O—Fe—O angles [108.0 (1) $\leq$ $\angle_{O-Fe-O}$ ≤ 113.0 (2)°] indicate slightly distorted tetrahedra (Table 3). The bending angles on the O atoms are 140.2 (2) $\leq$ $\angle_{Fe-O-Fe} \leq 149.8$ (2)°, and they differ distinctly from the ideal value (180°) reported for β-cristobalite, or *e.g.* for CsFeO₂. The size of the Fe—O—Fe angle depends on the effective

radii of the alkali metal cations and thus it increases continuously from β-NaFeO₂ (126°), KFeO₂ (135°), RbFeO₂ (144°) to CsFeO₂ (180°).
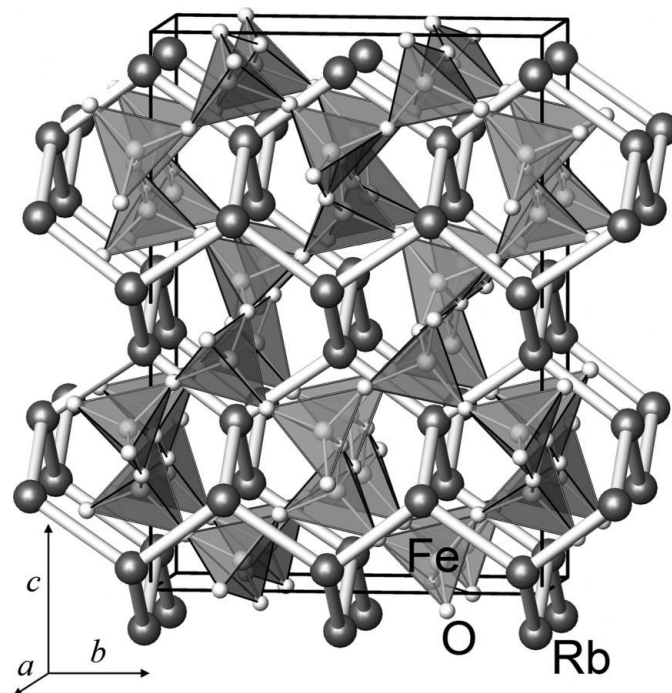
Figure 4
Crystal structure of RbFeO₂, with unit cell. The sticks between Rb atoms emphasize the diamond-like structure of Rb.
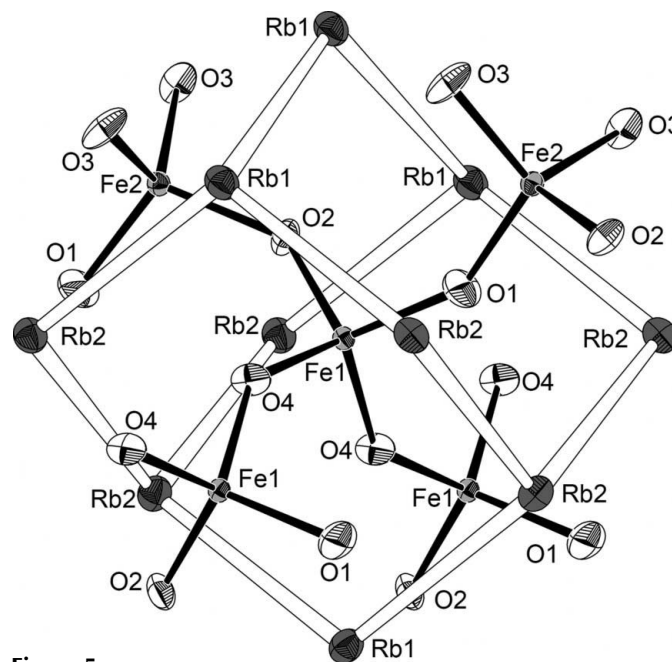
Figure 5
Fragment of the RbFeO₂ structure with atomic labeling scheme. The white sticks between Rb atoms emphasize the diamond-like structure of Rb, the black sticks are Fe—O bonds. Displacement ellipsoids are drawn at the 50% probability level.
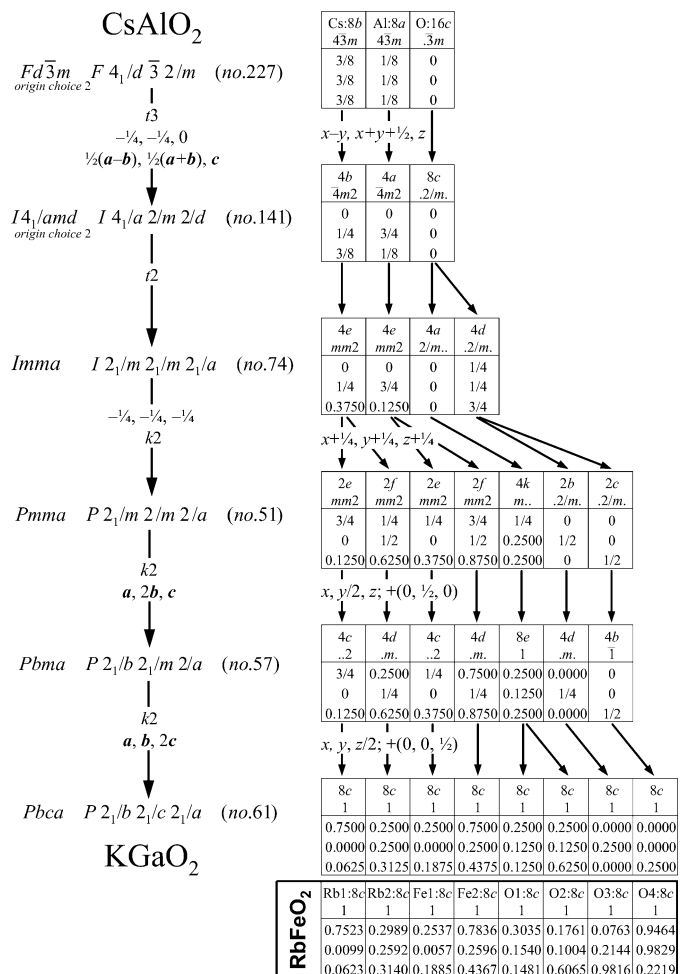
CsAlO₂

$Fd\bar{3}m$ ($F\,4_1/d\,\bar{3}\,2/m$) origin choice 2 (no.227)

Cs:8b	Al:8a	O:16c
43m	43m	.3m
3/8	1/8	0
3/8	1/8	0
3/8	1/8	0

| t3
−¼, −¼, 0
½(**a**−**b**), ½(**a**+**b**), **c**

$x-y,\ x+y+\tfrac{1}{2},\ z$

$I4_1/amd$ ($I\,4_1/a\,2/m\,2/d$) origin choice 2 (no.141)

4b	4a	8c
4̄m2	4̄m2	.2/m.
0	0	0
1/4	3/4	0
3/8	1/8	0

| t2

$Imma$ ($I\,2_1/m\,2/m\,2_1/a$) (no.74)

4e	4e	4a	4d
mm2	mm2	2/m..	.2/m.
0	0	0	1/4
1/4	3/4	0	1/4
0.3750	0.1250	0	3/4

−¼, −¼, −¼
k2

$x+\tfrac{1}{4},\ y+\tfrac{1}{4},\ z+\tfrac{1}{4}$

$Pmma$ ($P\,2_1/m\,2/m\,2/a$) (no.51)

2e	2f	2e	2f	4k	2b	2c
mm2	mm2	mm2	mm2	m..	.2/m.	.2/m.
3/4	1/4	1/4	3/4	1/4	0	0
0	1/2	0	1/2	0.2500	1/2	0
0.1250	0.6250	0.3750	0.8750	0.2500	0	1/2

k2
a, 2**b**, **c**

$x,\ y/2,\ z;\ +(0,\ \tfrac{1}{2},\ 0)$

$Pbma$ ($P\,2_1/b\,2_1/m\,2/a$) (no.57)

4c	4d	4c	4d	8e	4d	4b
..2	.m.	..2	.m.	1	.m.	1̄
3/4	0.2500	1/4	0.7500	0.2500	0.0000	0
0	1/4	0	1/4	0.1250	1/4	0
0.1250	0.6250	0.3750	0.8750	0.2500	0.0000	1/2

k2
a, **b**, 2**c**

$x,\ y,\ z/2;\ +(0,\ 0,\ \tfrac{1}{2})$

$Pbca$ ($P\,2_1/b\,2_1/c\,2_1/a$) (no.61)

8c	8c	8c	8c	8c	8c	8c	8c
1	1	1	1	1	1	1	1
0.7500	0.2500	0.2500	0.7500	0.2500	0.2500	0.0000	0.0000
0.0000	0.2500	0.2500	0.2500	0.1250	0.1250	0.2500	0.0000
0.0625	0.3125	0.1875	0.4375	0.1250	0.6250	0.0000	0.2500

KGaO₂

RbFeO₂

Rb1:8c	Rb2:8c	Fe1:8c	Fe2:8c	O1:8c	O2:8c	O3:8c	O4:8c
1	1	1	1	1	1	1	1
0.7523	0.2989	0.2537	0.7836	0.3035	0.1761	0.0763	0.9464
0.0099	0.2592	0.0057	0.2596	0.1540	0.1004	0.2144	0.9829
0.0623	0.3140	0.1885	0.4367	0.1481	0.6065	0.9816	0.2219

Figure 6
Group–subgroup relation between CsAlO₂ and KGaO₂, including the coordinates of RbFeO₂ and how they arise from those of the aristotype, CsAlO₂. Boxes shown contain: element, Wyckoff symbol, site symmetry and atomic coordinates x, y, z.

This structural feature is probably the reason for the twinning of the crystals under investigation. We assume a phase transition to occur at higher temperature from the KGaO₂ type of structure to the CsAlO₂ structure, with the Fe—O—Fe bending angle 144° seemingly approaching 180° because of librational disorder. The twinning is thus a result of the synthesis procedure at high temperatures and the subsequent cooling to room temperature (transformation twin). A comparable twinning phenomenon is also observed for the structurally related high/low phase transition of cristobalite. Below 500 K the cubic high-temperature modification (β-cristobalite) transforms into the tetragonal low-temperature modification (α-cristobalite) with three or six different twin domains present (Dollase, 1965; Peacor, 1972).

The group–subgroup relation (Wondratschek & Müller, 2004; Müller, 2004) between the aristotype CsAlO₂ and KGaO₂ includes two consecutive steps of symmetry reduction of the type *translationengleich* (t3 and t2, Fig. 6), which can be associated with multiple twinning in terms of 'twins by twins',[2] and resulting in six (3 × 2) twinning fractions, as observed. Fig. 6 shows the group–subgroup relation (*Bärnighausen–Stammbaum*), including all the site transformations. A comparison between the atomic coordinates of RbFeO₂ and the idealized values indicates that the major structural changes, in comparison to the CsAlO₂ structure, are caused by a shift of the O atoms, and to a lesser extent of Rb2 and Fe2.

We assume a phase transition of CsFeO₂ from the CsAlO₂ type of structure to the KGaO₂ structure also takes place, below room temperature. The bending angle should lock in at approximately 165° and crystals of CsFeO₂ at lower temperatures are expected to also be systematically twinned. A hint that gives support to this fact is provided by the relatively large displacement parameters determined for the O atoms at room temperature (Frisch & Röhr, 2004).

The twinning phenomena reported here are also related to the so-called *albite twinning* (Goldschmidt & Jenkins, 1985) in the sodium feldspar (NaAlSi₃O₈) caused by a displacive phase transition (collapse of the framework when the cation in the cavity site is too small) from high albite (monoclinic) into low albite (triclinic). This is in contrast to the *pericline twinning* in K-bearing alkali feldspar caused by an order–disorder phase transition at the Al/Si site (Xu *et al.*, 1995).

References

Barth, T. F. W. (1935). *J. Chem. Phys.* **3**, 323–325.
Bertaut, F. & Blum, P. (1954). *C. R. Acad. Sci.* **239**, 429–431.
Bruker AXS (2005). *Bruker Suite.* Bruker AXS Inc., Madison, WI, USA.
Cahn, R. W. (1954). *Adv. Phys.* **3**, 363–445.
Dollase, W. A. (1965). *Z. Kristallogr.* **121**, 369–377.
Dowty, E. (2005). *ATOMS*, Version 6.3. Shape Software, Kingsport, Tennessee, USA.
Frisch, G. & Röhr, C. (2004). *Z. Naturforsch. B*, **59**, 771–781.
Goldschmidt, J. R. & Jenkins, D. M. (1985). *Am. Mineral.* **70**, 911–923.
Hahn, Th. & Klapper, H. (2003). *International Tables for Crystallography*, edited by A. Authier, Vol. D, ch. 3.3, pp. 393–448. Dordrecht: The Netherlands: Kluwer Academic Publishers.
Henke, H. (2003). *Z. Kristallogr.* **218**, 617–625.
Hoppe, R. (1965a). *Angew. Chem.* **77**, 551.
Hoppe, R. (1965b). *Angew. Chem. Int. Ed. Engl.* **4**, 534–535.
Müller, U. (2004). *Z. Anorg. Allg. Chem.* **630**, 1519–1537.
Peacor, D. R. (1972). *Z. Kristallogr.* **138**, 274–298.
Pistorius, C. W. F. T. & de Vries, G. F. (1973). *Z. Anorg. Allg. Chem.* **395**, 119–121.
Sheldrick, G. M. (1997a). *SHELXS*97. University of Göttingen, Germany.
Sheldrick, G. M. (1997b). *SHELXL*97. University of Göttingen, Germany.
Sheldrick, G. M. (2007). *TWINABS*, Version 2007/3. University of Göttingen, Germany.
Smith, J. V. & Brown, W. L. (1988). *Feldspar Minerals*, Vol. 1, *Crystal Structures, Physical, Chemical, and Microtexture Properties*. Berlin, Germany: Springer Verlag.

---

[2] A term initially used by H. Bärnighausen for the reduction of symmetry in two consecutive steps of type translationengleich accompanied by multiple twinning due to a phase transition (Henke, 2003).

Sofin, M., Friese, K., Nuss, J., Peters, E.-M. & Jansen, M. (2002). *Z. Anorg. Allg. Chem.* **628**, 2500–2504.

Sofin, M., Peters, E.-M. & Jansen, M. (2002). *Z. Anorg. Allg. Chem.* **628**, 2697–2700.

Tabuchi, M., Ado, K., Kobayashi, H., Matsubara, I., Kageyama, H., Wakita, M., Tsutsui, S., Nasu, S., Takeda, Y., Masquelier, C., Hirano, A. & Kanno, R. (1998). *J. Solid State Chem.* **141**, 554–561.

Tomkowicz, Z. & Szytuła, A. (1977). *J. Phys. Chem. Solids*, **38**, 1117–1123.

Trinschek, D. & Jansen, M. (1999a). *Angew. Chem.* **111**, 234–235.

Trinschek, D. & Jansen, M. (1999b). *Angew. Chem. Int. Ed. Engl.* **38**, 133–135.

Vielhaber, E. & Hoppe, R. (1969). *Z. Anorg. Allg. Chem.* **369**, 14–32.

Wondratschek, H. & Müller, U. (2004). Editors. *International Tables for Crystallography*, Vol. A1. Dordrecht, The Netherlands: Kluwer Academic Publishers.

Xu, H., Veblen, D. R. & Luo, G. (1995). *Acta Cryst.* A**51**, 53–60.